Journal of Engineering and Applied Sciences 13 (24): 10364-10374, 2018
ISSN: 1816-949X

Preparation, Characterization of TiO_2 Nanoparticles by Electrodeposition Method and Using as Catalyst in Photocatalytic Degradation

[1]Hayder Khudhair Khattar, [2]Fouad Abdul Ameer Al-Saady and [1]Amer Mousa Jouda
[1]Faculty of Science, University of Kufa, Kufa, Iraq
[2]College of Pharmacy, Al-Mustansiriyah University, Baghdad, Iraq

Abstract: In order to get of catalyst inexpensive and effective application for photodegradation, TiO_2 powder which were prepared by the electrodeposition method simple and inexpensive and using surfactants such as (Glycerin (GLY), Polyvinyl Alcohol (PVA), Poly (N-Vinylpyrrolidone) (PVP)) that help the growth and nucleation of suspended particles. These particles were distinguished by (Atomic Force Microscopy (AFM), X-Ray Diffraction (XRD), Field Emission Scanning Electron Microscopy (FESEM), EDS and High Resolution Transmission Electron Microscope (HRTEM), these particle was obtained reached to the about 40 nm, in order to demonstrate the photodegradation efficiency of the titanium dioxide in the removal of the organic Malachite Green oxalate (MG) dye, the catalyst was used in both cases the standard Titanium Oxide (TiO_2, 80 vol% anatase +20 vol% rutile) from (US research nanomaterials, Inc) and prepared TiO_2 calcination at 700°C to converted from anatas phase to TiO_2 anatase/rutile phase and the parameters such as amount of catalyst, concentration of dye, pH of dye sol and temperature were calculated. Pseudo first order reactions according to, the Langmuir-Hinshelwood can be obtained from results photocatalytic reactions. Parameters such as: Energy activation (Ea), Enthalpy of activation (ΔH^0), entropy of activation (ΔS^0) and free energy of activation (ΔG^0) were calculated the activation energy equal to (56.73±1) and (37.49±1) kJ/mol for (MG) dye inpresence TiO_2 NPs in tow case standard and prepared, respectively.

Key words: Electrochemical deposition of TiO_2, photochemical processing, thermodynamic, kinetic, mechanism, nanoparticles

INTRODUCTION

Nanoparticles especially metal oxides like titanium and zinc oxides play a crucial role in degradation of dyes. Photocatalytic degradation is the process of degradation of toxic metals and an alternative biological degradation process (Byrne *et al*., 1998). The titanium dioxide has multiple crystallographic phases such as rutile and anatase phase. The rutile phase has fast recombination rate and excited only in visible light. But the anatase phase excited only at UV lights and slow recombination rate. The reason for the mixed production of two phases is used to increase the photocatalytic property of the titanium oxide (Hurum *et al*., 2003, 2005, 2006). Recently, variety of methods has been used for the synthesis of titanium dioxide nanoparticles such as aerosol pyrolysis, calcinations and surfactant based colloidal synthesis (Ahonen *et al*., 1999; Li and Ishigaki, 2001; Ding and Liu, 1997; Zhang *et al*., 2001; Yang *et al*., 2001; Chemseddine and Moritz, 1999; Yin *et al*., 2001; Chae *et al*., 2003).

MATERIALS AND METHODS

Experimental: This method is simple and useful for generating nanoparticles. This approach includes using two electrodes, anode and cathode plates made of Titanium (Ti) with high purity reaches to 99.99% with scale (2 cm width×3 cm length×1.5 mm thick) from (99% Fluka Analytical, Swiss) the two electrode rinsed by acetone with deionized water, the two electrodes are placed facing each to other in a vertical way with a distance 2 cm between anode and the counter electrode, the electrical cell that contains 100 mL Deionized Water (DW) obtained from (Faculty of Pharmacy, University of Kufa, Iraq). The electrolysis has been employed with the temperatures (60°C) with continuous various voltages, the current passed in the circuit has been monitored with a voltmeter. Additionally, the production of nanoparticles in a way of electrochemical reduction in changing the polarity of the direct current between the electrodes during electrolysis process in order to obtund the better precipitation (Liao *et al*., 2000). Electrolyte was used to preparing TiO_2 NPs (0.745 g/100 mL, 1 M) KCl (99%

Corresponding Author: Hayder Khudhair Khattar, Faculty of Science, University of Kufa, Kufa, Iraq

Table 1: Chemical, solutions and working conditions applied in the experiment of TiO_2 NPs powder electrodeposition of KCl solutions

----------Chemicals----------		PVP	PVA	Glycerin
KCl	0.74 (g/100 mL)	1 M	1 M	1 M
Deionized water	0.7 (μsec/cm)	0.7 (μsec/cm)	0.7 (μsec/cm)	0.7 (μsec/cm)
Glycerin	(1g/100 mL)	-	-	10 (mL)
PVA	(1g/100 mL)	-	10 (mL)	-
PVP	(1g/100 mL)	10 (mL)	-	-
pH	7	7	7	7
Temperature	50-60°C	50-60°C	50-60°C	50-60°C
General current density	500 (A/m^2)	500 (A/m^2)	500 (A/m^2)	500 (A/m^2)
(Titanium) anode area	12 (cm^2)	12 (cm^2)	12 (cm^2)	12 (cm^2)
Current density	0.6 (A)	0.6 (A)	0.6 (A)	0.6 (A)
Voltage-time	(V)/(min)	19.2 (V)/60 (min)	17.1 (V)/60 (min)	18.3 (V)/60 (min)

Thomas, India) at pH (7). A power supply under study, DC applied by power supply (potentiostat/galvanostat) (China) was utilized to supply and measurement with more precision current additives like Glycerin (GLY), Polyvinyl Alcohol (PVA), Poly (N-Vinylpyrrolidone) (PVP) (CDH-India), material listed in Table 1. Afterwards, the white color of titanium dioxide powder was washed repeatedly with deionized water numerous times by using centrifugal (4000 rpm) several time and then wash twice with 99% ethanol and then dry in an oven 60°C for 1 h, latter store the deposited TiO_2 in tightly blocked vials, store in a vacuum container contain a silica gel powder (Murray *et al*., 2005).

RESULTS AND DISCUSSION

AFM measurements of TiO_2 powder electrodeposition: The AFM analysis of precipitated TiO_2 powder shows in Table 2 that the root mean square roughness (sq) is 9.73 nm, i.e, the surface roughness of TiO_2 with stabilizer glycerin which has packs with more heights than other sample with deferent stabilizer such as PVP and PVA, the results accordingly the roughness profile as the following, TiO_2 with glycerin >PVP>PVA, surface roughness of samples depends on operating conditions.

It was found that the average granulity cumulation distribution of diameter for nanoparticles TiO_2. When using 10 mL of PVP is 61.37 nm, the parameters are also, listed as (Fig. 1-3a-c) in Table 2 where it is clear that the sample is prepared with PVA>Glycerin>PVP (Gadelmawla *et al*., 2002).

X-ray measurements of TiO_2 powder electrodeposition: The purity and crystal phases of TiO_2 nanopowder were examined by X-ray diffraction, XRD data come from using a Shimadzu 6000 diffractometer equipped with Cu Kα radiation (λ = 1.5406 Å) (at 50 kV and 40 mA) in a scan range (2θ) from 20°-80° shows the XRD patterns for titanium dioxide nanoparticles which were nancrystalline in nature of TiO_2 which prepared by electrodeposition at room temperature, XRD patterns of the as-prepared samples with different conditions were shown in Fig. 4a is found to be crystalline and possesses anatase structure as it shows few peaks of anatase (101) and (004), X-ray diffraction analysis reveal that TiO_2 nanopowder are amorphous if the temperature sample is lower than 300°C (Yahya, 2010).

The diffraction peaks are in good agreement with those given in JCPD data card (JCPDS No. 21-1272 and 21-1276) for TiO_2 anatase and rutile as shown in Fig. 4 a, b. It is observed that the intensities of the peaks of few TiO_2 planes increased slightly with the increase of annealing temperature. In addition, the location of the (101) peaks is shifted to lower 2θ angles from 2θ = 25.27° to 2θ = 25.11°. The pronounced anatase TiO_2 characteristic diffraction peaks 2θ = 25.25° (101) and 48.0° (200) were found in the patterns, all the peaks in the XRD patterns can be indexed as anatase and rutile phases of TiO_2 and the diffraction data are in good agreement with data reported by Vijayalakshmi and Rajendran (2012) (Chen *et al*., 2004). From Fig. 4b, the X-ray diffraction patterns of the optimum TiO_2 NPs prepared by using electrochemical method have been TiO_2 prepared. It has been calcination to a temperature of 700°C to convert from TiO_2 anatas amorphous phase to crystallized phase TiO_2 anatas/rutile that corresponds to the standard sample shown in Fig. 5, used in photodegradation process.

SEM, TEM and EDS measurements of TiO_2 (NPs) electrodeposition with GLY, PVP, PVA: The SEM micrograph of the prepared TiO_2 nanoparticles, spherical and uniformly distributed particles can be seen, largest particles in figure may be aggregates from smaller particles (Reddy *et al*., 2010). The value of particle size observed in SEM and TEM image, good agreement with the results obtained from XRD, significantly important of spherical shape not only for the design of surface area and surface properties but also for accuracy the electronic structure, for visible light spectrum more active for photocatalytic activity better by observing SEM an image, we find nanoparticles distributed regularly in the shape of

Table 2: AFM measurements of TiO_2 powder electrodeposition of KCl solutions by using PVA, Glycerin

CSPM imager surface roughness analysis (amplitude parameters)

TiO_2	PVP	PVA	Glyserin
Roughness average (sa) nm	2.3400	0.5680	8.4300
Root mean square (sq) nm	2.7800	0.6560	**9.7300**
Surface skewness (Ssk)	-0.2330	-0.0543	**0.0319**
nm surface kurtosis (sku) nm	**2.1100**	1.8400	1.8100
Sku = (3) mesokurtic, <(3) liptokurtic, >(3) platykurtic	**2.1100**>	1.8400>	1.8100
Peak-peak (sy) nm	11.100	3.0700	34.100
Ten point height (sz) nm	11.100	2.8500	34.100
Hybrid parameters			
Mean summit curvature) ssc (1/nm)	-0.0107	-0.0023	-0.0430
Root mean square slope (sdq) (1/nm)	0.1790	0.0390	0.6440
Surface area ratio (sdr)	1.5800	0.0767	18.700
Functional parameters			
Surface bearing index (sbi)	4.4900	1.2000	4.3000
Core fluid retention index (sci)	1.3900	1.4600	1.5100
valley fluid retention index (svi)	0.1100	0.0744	0.0666
Reduced summit height (spk) nm	0.2810	0.1330	4.6000
Core roughness depth (sk) nm	8.5700	2.1200	28.3000
Reduced valley depth (svk) nm	2.0700	0.1840	1.1600
Spatial parameters			
(density of summits) Sds (1/um^2)	335.00	277.00	366.00
Fractal dimension	2.1200	2.7000	2.1100
Avg. diameter nm	61.37	103.45	69.27
Voltage (V)	19.2	17.1	17.9

Bold values are significant

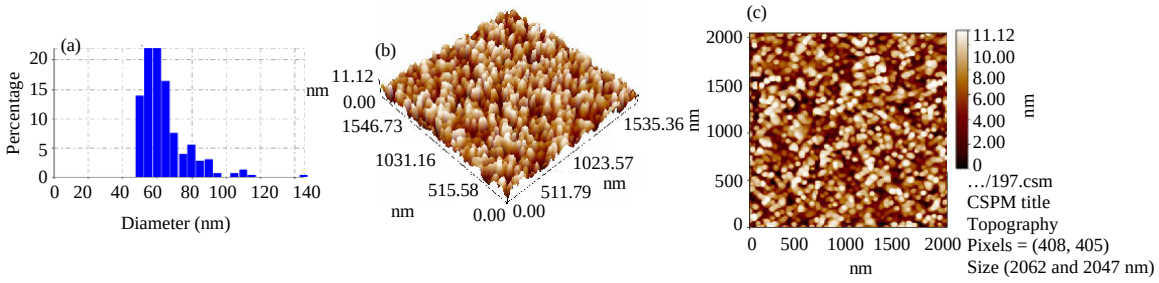

Fig. 1: AFM images of TiO_2 powder electrodeposition of KCl solutions with PVP (10 mL). Avg. diameter: 61.3 nm: a) Granulity cumulation distribution chart; b) 3-Dimensinal image and c) 2-Dimensional image

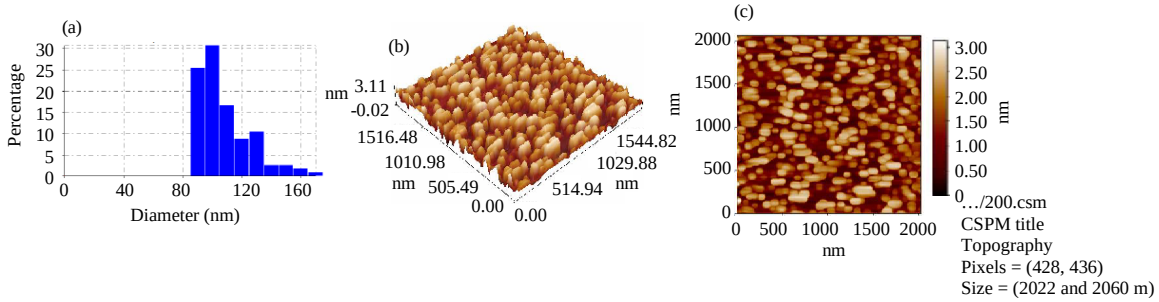

Fig. 2: AFM images of TiO_2 powder electrodeposition of KCl solutions with PVA (10 mL). Avg. diameter 103.45 nm: a) Granulity cumulation distribution chart; b) 3-Dimensinal image and c) 2-Dimensional image

circular spherical particles, spherical in shape and without aggregation (Fig. 6) (Narayana *et al*., 2011). The TEM image of TiO_2 appear spherical for all particles, narrow shape and distribution is displayed with a size of 40-80 nm. The EDs was recorded in the binding energy region of 0-15 keV is shown in Fig. 6-8. The spectrum peak is reveal the atomic % of Ti and O, the present composition of Ti and O reveals that, the formation of non-stoichiometric TiO_2 which is superior for photocatalytic applications.

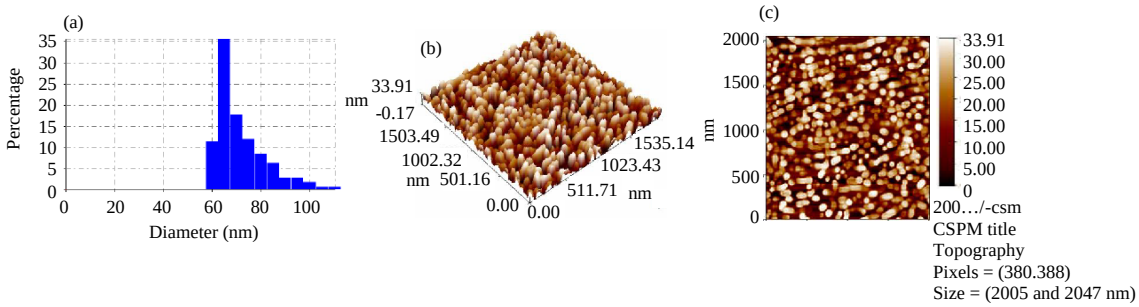

Fig. 3: AFM images of TiO_2 powder electrodeposition of KCl solutions with GLY (10 mL). Avg. diameter: 69.27 nm: a) Granulity cumulation distribution chart; b) 3-Dimensinal image and c) 2-Dimensional image

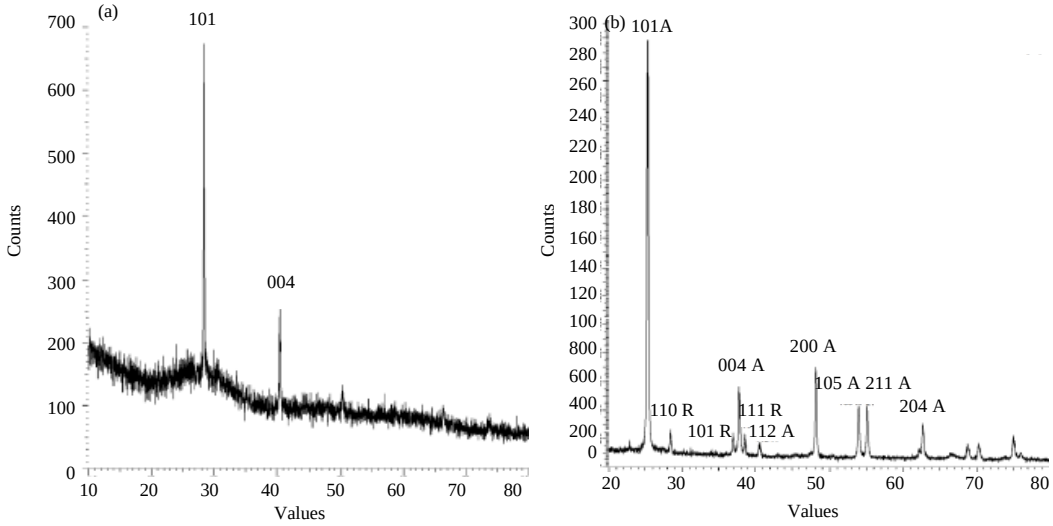

Fig. 4: X-ray images of TiO_2 nanopwoder amorphous phase: a) Calcination at 700°C for 1 h and b) Electrodeposition of KCl solutions

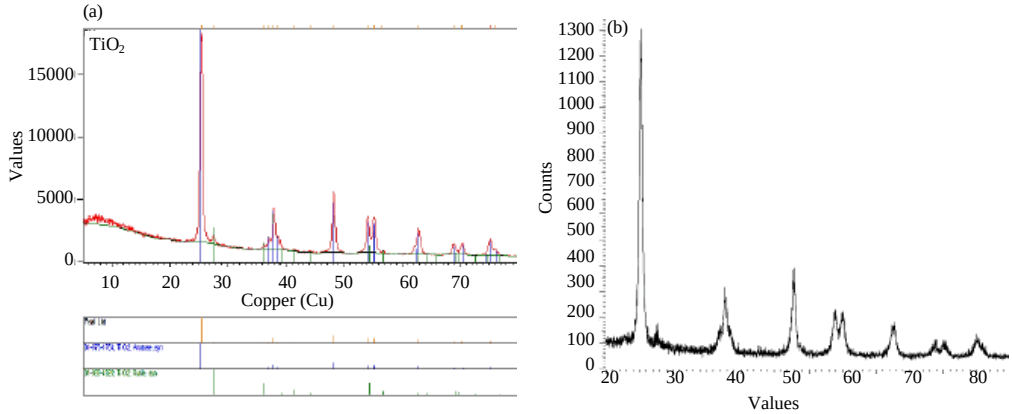

Fig. 5: X-ray images of TiO_2 nanopwoder (anatase/rutile) standard, from USA, US Research Nanomaterials, Inc

Photodegradation of MG by TiO_2 as catalyst: In order to prove the potential of TiO_2 oxide from electrical way as a catalyst in the destruction of organic pollutants from pigments, wastewater or textile plants and to the increasing demand for highly efficient and inexpensive catalysts, Malachite Green oxalate (MG) dye under studied with absorption about (617 nm) and good stability with visible light (Jiang *et al*., 2015). MG which is specific

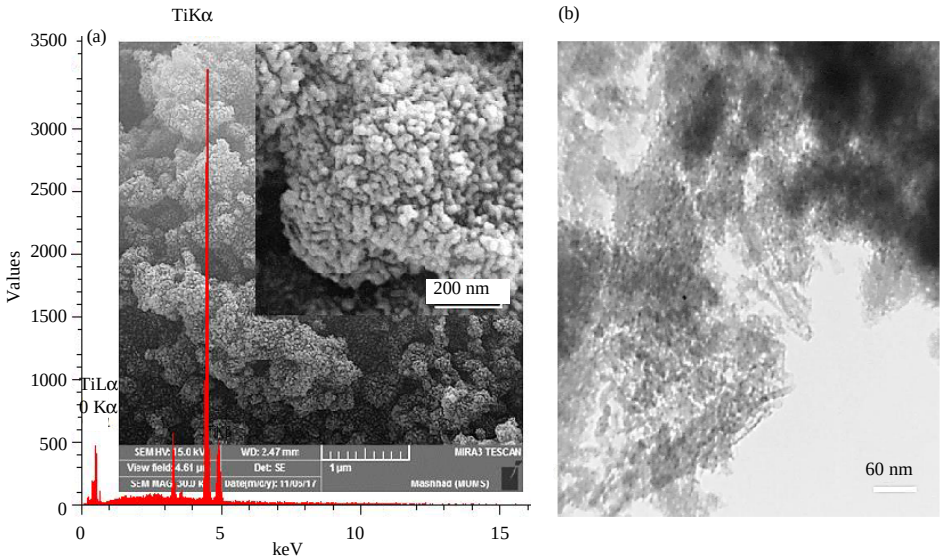

Fig. 6a, b: SEM, TEM and EDS images of TiO_2 NPs electrodeposition in KCL (0.1) M with GLY (10 mL), vigorous stirring (Ti = 30.25 wt.%, O = 69.75 wt.%)

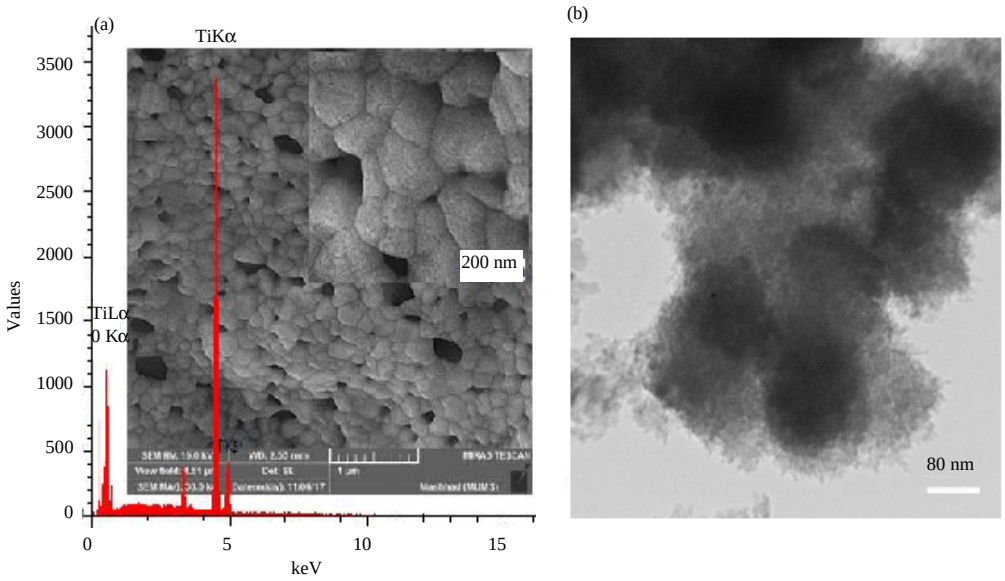

Fig. 7a, b: SEM , TEM and EDS images of TiO_2 NPs electrodeposition in KCL (0.1) M with PVA (10) mL, vigorous stirring (Ti = 35.53 wt.%, O = 64.47 wt.%)

as a basic dye which is an great water soluble dye relationship to triphenylmethane family M.wt. 927.01 g/mol (Alderman, 1985; Sawa and Hoten, 2001; Vijayalakshmi and Rajendran, 2012; Culp *et al*., 1999). The homely photoreactor equipment mercury lamp-Philips-Holland (250 W) without cover glass as a source for UV irradiation (Shimadzu UV 1650 PC Japan) was used to decide the declination degree of the (MG) dye solutions (LAB) tech, hot plate Korea. The space of lamp and solution glass is 15 cm. The test occur at 25°C and closed compartment to block escape of harmful radiation the suspension pH values were adjusted at desired level using (0.01) N NaOH or (0.01) N HCl solutions were measured via. pH meter-Hanna tool, the water mixture was stirred magnetically during the amount of dye adsorbed and reduced was determined by change in the absorbance of (MG) dye using Eq. 1:

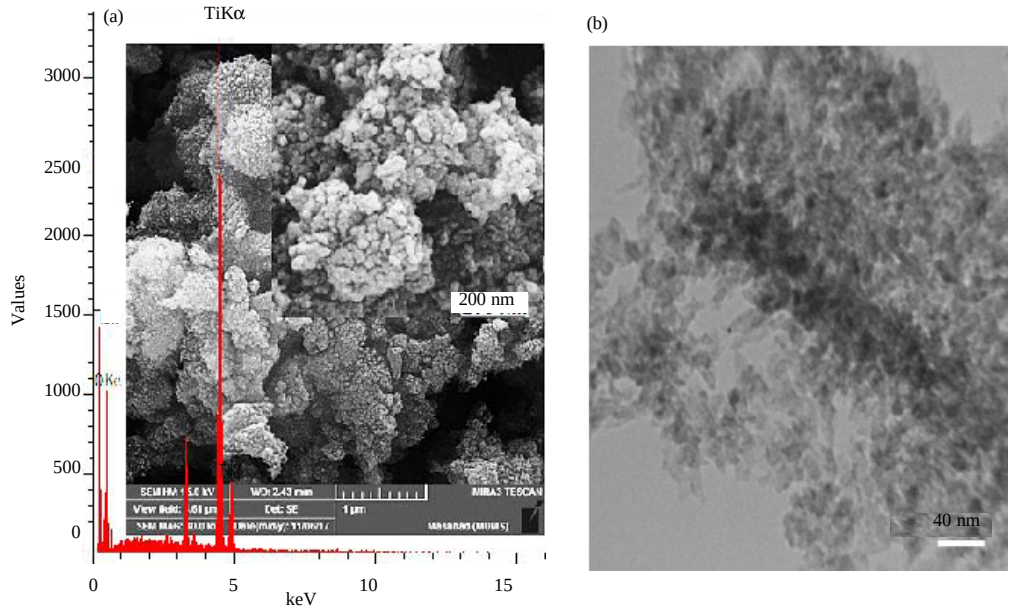

Fig. 8a, b: SEM, TEM and EDS images of TiO_2 NPs electrodeposition in KCL (0.1) M with PVP (10) mL, vigorous stirring (Ti = 52.84 wt.%, O = 47.16 wt.%)

$$(D\%) = \left[\frac{C_o - C_a}{C_o}\right] \times 100\% \quad (1)$$

Where:

D% = The Degradation ratio

C_o = The initial Concentration of dye solution

C_a = The Concentration of dyes after adsorption by the catalyst

Dark reaction of MG dye in presence TiO_2 catalyst: In dark reaction performed tests in the lack of ultraviolet beam employ TiO_2 as a catalyst as show in Fig. 9, no deterioration in the loss of ultraviolet ray as results show where gave adding stimulation a slight change in the dye concentration in an incubation time slightly pigment concentrations decrease, after limited period of time. It becomes fixed where the monolayer configuration on the surface of the catalyst because no active sites useful for extra adsorption, so, no additional lessening in dye concentrations was observed. Thus, the yield obtained of the absorption taste confirm the low concentration of solutions (MG) is due to the absorption of dyes over catalysts, then no degradation of dyes was found. The conclusion show that the balance occurs after (90 min). The percentage of decomposition efficiency is calculated at (29.05 and 39.425%) for the TiO_2 (standard, prepared calcination at 700°C), respectively.

Photodegradation of MG dye solution by UV irradiation in catalyst absence: The photodegradation of MG dye solution by UV irradiation in catalyst absence as in Fig. 10

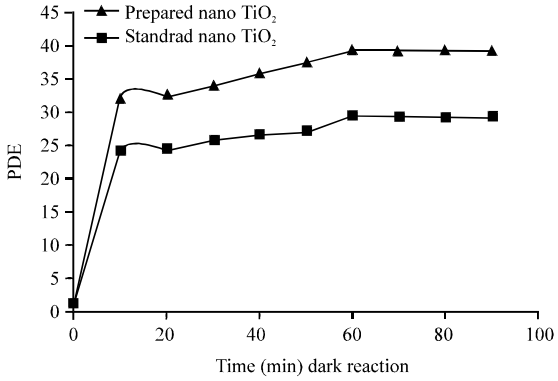

Fig. 9: The degradation efficiency of MG with (standard anatase/rutile, prepared anatase/rutile calcination at 700°C from TiO_2 catalyst, absence the UV radiation

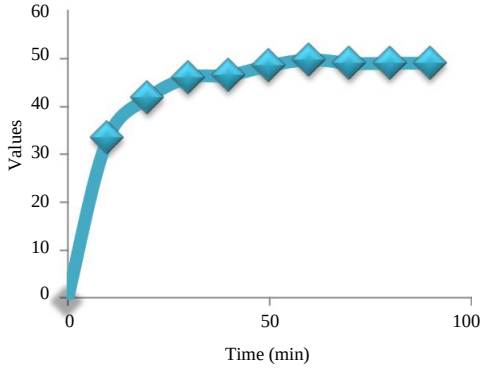

Fig. 10: The photodegradation efficiency of MG dyes without the catalyst

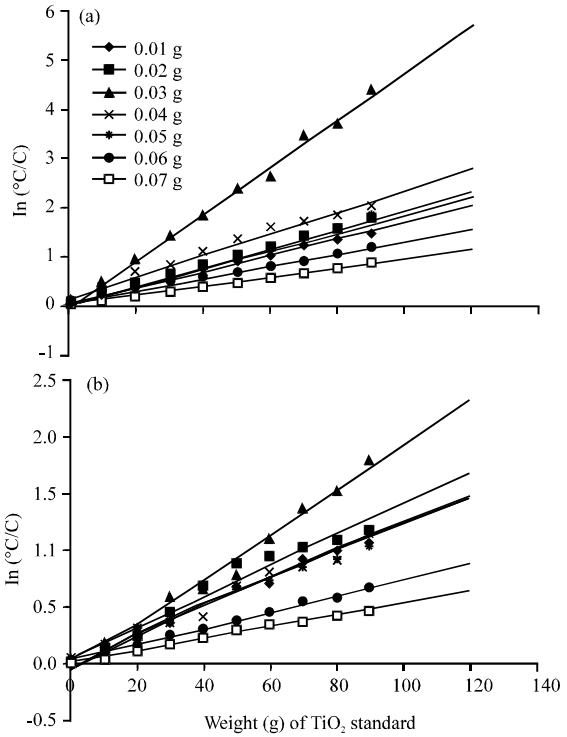

Fig. 11a): Effect of weight of TiO_2 (standard) on photodegradation efficiency of MG and b) Effect of weight TiO_2 (prepared) on photodegradation efficiency of MG

can be determined result after 90 min of UV treating, the Photodegradation Efficiency (PDE %) can be observed (49.75%) take effect by the ultraviolet radiation in catalyst absence.

Effect of TiO_2 mass on the rate of degradation of MG dye: The influence of amount catalyst onto photocatalytic degradation for MG dyes, light power (250 W) at (25°C) and variable the mass of TiO_2 NPs for both (standard, prepared) in range (0.01-0.07) g in 100 mL from 4 ppm of MG dye. If the concentration of photocatalyst crosses certain optimum value in the suspension then the penetration of light through the suspension reduces that causes decrease in the rate of decolourization of dye (Kartal *et al*., 2001; Neppolian *et al*., 2002). Thus, for executing any continuous research, the catalyst dose optimization is required before starting any photolysis process. Through Fig. 11a, b, for TiO_2 NPs for both (standard, prepared). The following is illustrated, the best weight of TiO_2 is 0.03 for tow catalyst. Photodegradation efficiency for TiO_2 NPs for both (standard, prepared) which is equal to 98.74 and 83.2%, respectively.

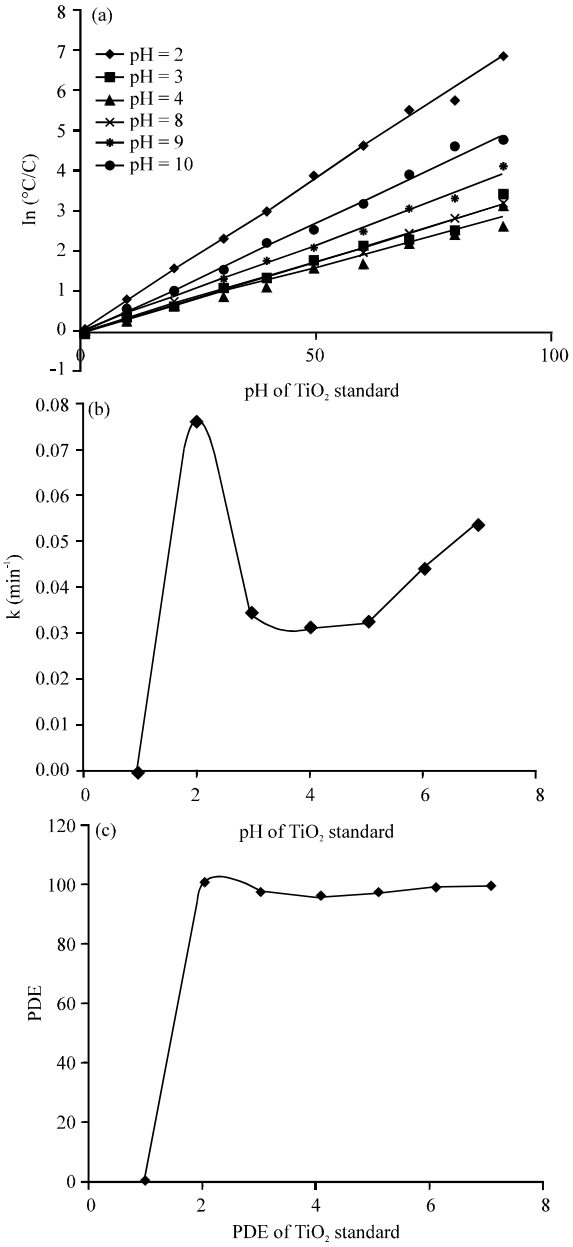

Fig. 12a-c): Influence of pH on photocatalytic degradation efficiency of MG with 0.03 g TiO_2 (standard)

Effect pH of TiO_2 on the rate of degradation of MG dye: By studying the changes in pH solution in the range of 2-10 by maintaining other test conditions fixed, dye concentration of 4 ppm, light power (250 W), catalyst dose (0.03) g, at (25°C). The results observed in Fig. 12a, b. The influence of the initial solution pH on the removal of MG by TiO_2 NPs, TiO_2 is amphoteric in aqueous solution (Neppolian *et al*., 2002), the higher the

Table 3: The values of rate constant, kinetics and thermodynamic parameters for the photocatalytic degradation of MG dye at (303-318) K with (0.03) g of TiO_2 standard, prepared)

		K (sec^{-1})×10^{-5}		ln K		Ea (kJ/mol)		ΔH^0 (kJ/mol)		ΔS^0 (kJ/mol/k)		ΔG^0 (kJ/mol)	
T (k°)	1\T	TiO_2 prepared	TiO_2 standard	TiO_2 prepared	TiO_2 standard	TiO_2 prepared	TiO_2 standard	TiO_2 prepared	TiO_2 standard	TiO_2 prepared	TiO_2 standard	TiO_2 prepared	TiO_2 standard
303	0.00330	4.166	4.330	-10.085	-10.047	-	-	34.979	54.215	-	-	96.488	96.029
308	0.00324	5.833	9.166	-9.749	-9.297	-	-	34.937	54.174	-	-	97.461	96.719
313	0.00319	7.660	12.200	-9.476	-8.987			34.896	54.132	-	-	98.435	97.409
318	0.00314	11.160	18.600	-9.100	-8.589			34.854	54.090	-	-	99.408	98.099

dissolution rate of the pollutant was observed at higher the acidic reaction medium than the neutral and basic mean, increased catalyst effectiveness can be explained when the medium is acidic because the catalyst surface is positively charged, this leads to the attraction of pollutant-negative aggregates to the surface of the catalyst and increases adsorption, thereby, increasing the disintegration of the pollutant as well as increasing the attraction of negative hydroxyl ions that can be transformed into the free hydroxyl radical caused by hole that are responsible for the disintegration of the pollutant, it can be seen that the adsorption percentage maintained very high (99.89%), (90.49%) at pH = (2) and (99.15%), (89.38 %) at pH = (10), for both TiO_2 NPs (standard, prepared), respectively.

Effect of MG dye concentration on the rate of degradation in presence TiO_2 NPs: The influence of primary dye concentration on the photocatalytic degradation rate can be calculated by maintenance all other test conditions stable at light power (250 W), the pH = (2) at (25°C), (0.03) g for TiO_2 NPs for both (standard, prepared) and changing the primary dye concentration in domain (1-7) ppm as in form Fig 13a, b, the results show that with the reduced concentration of the dye, the rate of photo degradation increases this is because increasing the concentration of the primary dye reduces the length of the photon path into the solution, thereby, reducing the number of photons reaching the catalyst surface and hence, rate of formation hydroxyl radicals and super oxide ions (O^{2-}) is reduce because of the lower surface area exposed to the excitation, the rate of photolysis decreases (Hustert and Zepp, 1992; Daneshvar *et al*., 2008.

Effect of temperature on photocatalytic degradation efficiency of MG dye with 0.03 g TiO_2 catalyst: In range of temperature (303-318) K, the effect of temperature on dye removal was studied by keeping other experimental conditions constant at dye concentration of 1 ppm, light intensity equal to 250 W, TiO_2 for both (standard, prepared) catalyst dosage was 0.03 g, pH dye solution equal to (2) as in Fig 14a,b, the results are listed in Table 3, the temperature is directly proportional to the disintegration of the pollutant where the photodegradation is increased by increasing the reaction temperature.

Thermodynamic, kinetic studied of plot ln (k) vs. 1/T: Experimental data obtained through thermodynamic investigation were analyzed. Thermodynamic parameters such as standard free energy change (ΔG°, kJ/mol), thermal content change (ΔH°, kJ/mol) and entropy change (ΔS°, kJ/mol/k) were determined expressed in Eq. 2-4:

$$\ln A = \ln\frac{KBT}{h} + \frac{\Delta S^0}{R} \quad (2)$$

$$\Delta G^0 = \Delta H^0 - T\Delta S^0 \quad (3)$$

$$\Delta H^0 = E_a - RT \quad (4)$$

Brief the thermodynamic parameters determined at different temperatures ranging from (303-318) K. The positive value of ΔH^0 substantiated the endothermic nature of the dye sorption process. The negative ΔS^0 values suggest the decreased randomness at solid-liquid interface and reflect favorable condition for the removal MG dyes from solutions. These results indicate that the degradation efficiency not significantly affected with the increase of temperature, according to MG reduced the rate of most reactions varies with temperature in such a way that:

$$k = Ae^{-Ea/RT} \quad (5)$$

The activation energy E_a was calculated from the Arrhenius plot of lnk vs. 1/T the slope of linear plot is equal to $-E_a/R$ as show in Fig. 15a, b, the entropy of activation ΔS^0 was calculated from Eq. 2 (Daneshvar *et al*., 2008). The activation energy for photodegradation and decontamination in MG solution using the titanium dioxide catalyst in the (303-318) K temperature range was (56.734±1) and (37.498±1) kJM^{-1}, respectively.

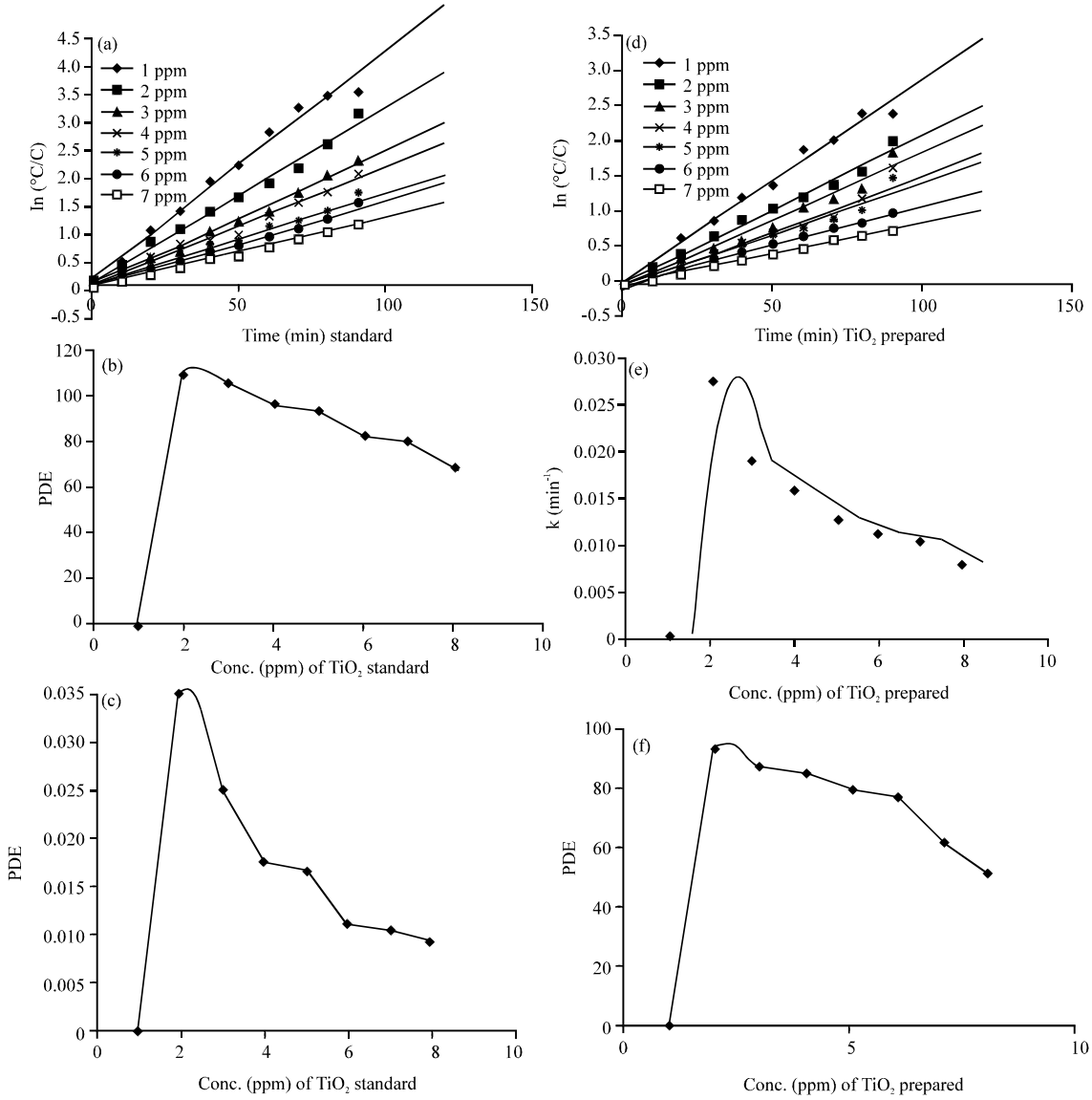

Fig. 13a-c): The variable in photocatalytic degradation efficiency for MG dye with concentration in presence (0.03) g of TiO_2 (standard) and d-f) The variable in photocatalytic degradation efficiency for MG dye with concentration in presence (0.03) g of TiO_2 (prepared)

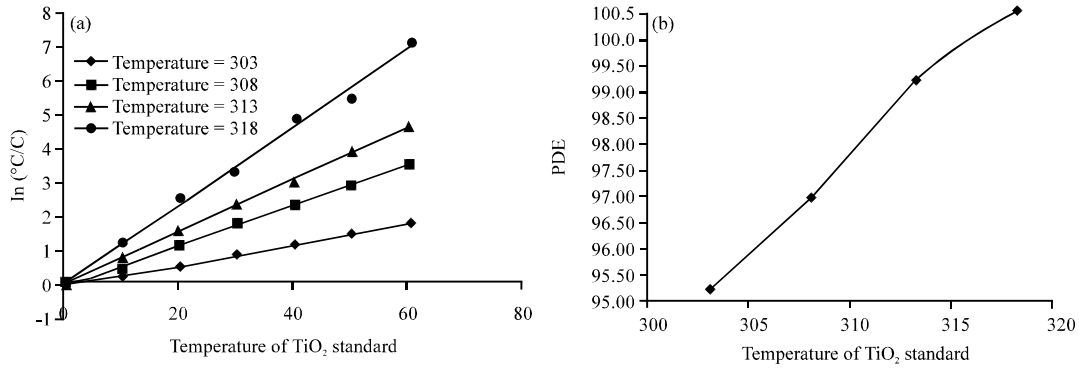

Fig. 14: Continue

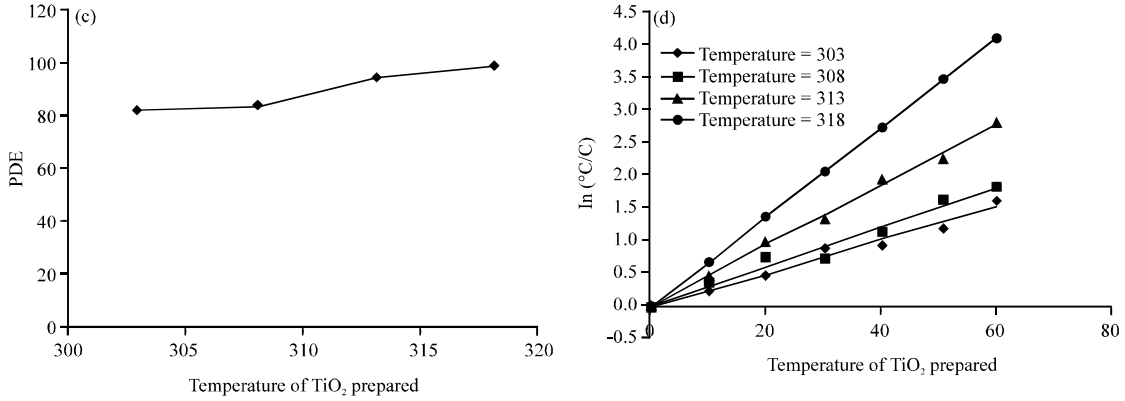

Fig. 14a, b): Effect of temperature on photocatalytic degradation efficiency of MG dye with 0.03 g TiO_2 standard and c-d): Effect of temperature on photocatalytic degradation efficiency of MG dye with 0.03 g TiO_2 prepared

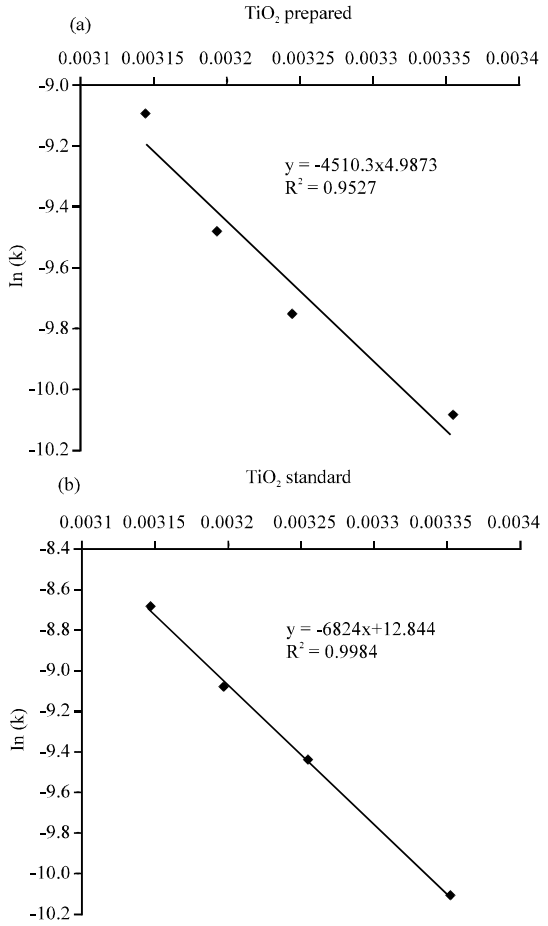

Fig. 15a, b): Arrhenius plot of MG dye (0.03) g TiO_2 standard and prepared

CONCLUSION

By electrochemical can be prepared successfully TiO_2 nanoparticles, inexpensive, simple and high-precision way to control the size and shape of the nanometer. To improve the catalytic performance of photocatalysis and to increase crystallization, the prepared powder was calcination to 700°C, to converted from anatas phase to TiO_2 anatase/rutile phase, for comparison with standard Titanium Oxide (TiO_2, 80 vol% anatase+20 vol% rutile) from (US research nanomaterials, Inc), the result indicates that (E_a) which was referred to as 56.73, 37.49 for both prepared and standard, respectively, the thermodynamic parameters of the degradation of MG solutions and titanium oxide refer to the positive ΔH^0 certain on endothermic reaction, the positive ΔG^0 result indicate that the non-spontaneous reaction, entropy of activation ΔS^0 is negative less randomly, the reactive species such as hydroxyl radical and superoxide anion have been produced from the heterogeneous photocatalytic reaction. The results of the fragmentation of the dye by the catalyst were CO_2 and H_2O.

REFERENCES

Ahonen, P.P., E.I. Kauppinen, J.C. Joubert, J.L. Deschanvres and V.G. Tendeloo, 1999. Preparation of Nanocrystalline Titania powder via aerosol pyrolysis of Titanium Tetrabutoxide. J. Mater. Res., 14: 3938-3948.

Alderman, D.J., 1985. Malachite green: A review. J. Fish Dis., 8: 289-298.

Byrne, J.A., B.R. Eggins, N.M.D. Brown, B. McKinney and M. Rouse, 1998. Immobilisation of TiO_2 powder for the treatment of polluted water. Appl. Catal. B. Environ., 17: 25-36.

Chae, S.Y., M.K. Park, S.K. Lee, T.Y. Kim and S.K. Kim *et al*., 2003. Preparation of size-controlled TiO_2 nanoparticles and derivation of optically transparent photocatalytic films. Chem. Mater., 15: 3326-3331.

Chemseddine, A. and T. Moritz, 1999. Nanostructuring Titania: Control over nanocrystal structure, size, shape and organization. Eur. J. Inorg. Chem., 1999: 235-245.

Chen, C.C., C.S. Lu, Y.C. Chung and J.L. Jan, 2007. UV light induced photodegradation of malachite green on TiO_2 nanoparticles. J. Hazard. Mater., 141: 520-528.

Culp, S.J., L.R. Blankenship, D.F. Kusewitt, D.R. Doerge and L.T. Mulligan *et al*., 1999. Toxicity and metabolism of Malachite green and Leucomalachite green during short-term feeding to Fischer 344 rats and B6C3F1 mice. Chem. Biol. Interact., 122: 153-170.

Daneshvar, N., S. Aber and F. Hosseinzadeh, 2008. Study of CI acid orange 7 removal in contaminated water by photo oxidation processes. Global Nest J., 10: 16-23.

Ding, X.Z. and X.H. Liu, 1997. Synthesis and microstructure control of nanocrystalline titania powders via a sol-gel process. Mater. Sci. Eng. A., 224: 210-215.

Gadelmawla, E.S., M.M. Koura, T.M.A. Maksoud, I.M. Elewa and H.H. Soliman, 2002. Roughness parameters. J. Mater. Process. Technol., 123: 133-145.

Hurum, D.C., A.G. Agrios, K.A. Gray, T. Rajh and M.C. Thurnauer, 2003. Explaining the enhanced photocatalytic activity of degussa P25 mixed-phase TiO_2 using EPR. J. Phys. Chem. B., 107: 4545-4549.

Hurum, D.C., A.G. Agrios, S.E. Crist, K.A. Gray and T. Rajh *et al*., 2006. Probing reaction mechanisms in mixed phase TiO2 by EPR. J. Electron. Spectrosc. Rel. Phenom., 150: 155-163.

Hurum, D.C., K.A. Gray, T. Rajh and M.C. Thurnauer, 2005. Recombination pathways in the Degussa P25 formulation of TiO_2: Surface versus lattice mechanisms. J. Phys. Chem. B., 109: 977-980.

Hustert, K. and R.G. Zepp, 1992. Photocatalytic degradation of selected azo dyes. Chemosphere, 24: 335-342.

Jiang, W., X. Wang, Z. Wu, X. Yue and S. Yuan *et al*., 2015. Silver oxide as superb and stable photocatalyst under visible and near-infrared light irradiation and its photocatalytic mechanism. Ind. Eng. Chem. Res., 54: 832-841.

Kartal, O.E., M. Erol and H. Oguz, 2001. Photocatalytic destruction of phenol by TiO_2 powders. Chem. Eng. Technol., 24: 645-649.

Li, Y.L. and T. Ishigaki, 2001. Synthesis of crystalline micron spheres of Titanium Dioxide by thermal plasma oxidation of Titanium Carbide. Chem. Mater., 13: 1577-1584.

Liao, X.H., J.J. Zhu, X.N. Zhao and H.Y. Chen, 2000. Synthesis of Silver Nanoparticles by electrochemical method. Chem. J. Chin. Univ. Chin., 21: 1837-1839.

Murray, B.J., Q. Li, J.T. Newberg, E.J. Menke and J.C. Hemminger *et al*., 2005. Shape-and size-selective electrochemical synthesis of dispersed Silver (I) Oxide Colloids. Nano Lett., 5: 2319-2324.

Narayana, R.L., M. Matheswaran, A.A. Aziz and P. Saravanan, 2011. Photocatalytic decolourization of basic green dye by pure and Fe, Co doped TiO_2 under daylight illumination. Desalination, 269: 249-253.

Neppolian, B., H.C. Choi, S. Sakthivel, B. Arabindoo and V. Murugesan, 2002. Solar/UV-induced photocatalytic degradation of three commercial textile dyes. J. Hazard. Mater., 89: 303-317.

Reddy, M.V., R. Jose, T.H. Teng, B.V.R. Chowdari and S. Ramakrishna, 2010. Preparation and electrochemical studies of electrospun TiO_2 nanofibers and molten salt method nanoparticles. Electrochimica Acta, 55: 3109-3117.

Sawa, Y. and M. Hoten, 2001. Antibacterial activity of basic dyes on the dyed acrylic fibers. Sen. I Gakkaishi, 57: 153-158.

Vijayalakshmi, R. and V. Rajendran, 2012. Synthesis and characterization of nano-TiO_2 via different methods. Arch. Appl. Sci. Res., 4: 1183-1190.

Yahya, K., 2010. Characterization of pure and dopant TiO_2 thin films for gas sensors applications. Ph.D Thesis, Department of Applied Science, University of Technology, Lahore, Pakistan.

Yang, J., S. Mei and J.M. Ferreira, 2001. Hydrothermal synthesis of Nanosized Titania powders: Influence of Tetraalkyl Ammonium hydroxides on particle characteristics. J. Am. Ceram. Soc., 84: 1696-1702.

Yin, H., Y. Wada, T. Kitamura, S. Kambe and S. Murasawa *et al*., 2001. Hydrothermal synthesis of nanosized anatase and rutile TiO2 using amorphous phase TiO_2. Mater. Chem., 11: 1694-1703.

Zhang, H., M. Finnegan and J.F. Banfield, 2001. Preparing single-phase Nanocrystalline Anatase from Amorphous Titania with particle sizes tailored by temperature. Nano Lett., 1: 81-85.